INTERNATIONAL JOURNAL OF HYDROGEN ENERGY 44 (2019) 3021–3030

Available online at www.sciencedirect.com

ScienceDirect

journal homepage: www.elsevier.com/locate/he

Code development for analyzing transient behaviors induced by the in-box LOCA of liquid blanket in hydrogen fusion energy systems

Zi Meng [a], *Shichao Zhang* [a,b], *Zhibin Chen* [a,*], *Shisheng Wang* [a], *Changjian Wang* [c]

[a] *Key Laboratory of Neutronics and Radiation Safety, Institute of Nuclear Energy Safety Technology, Chinese Academy of Sciences, Hefei, Anhui, 230031, China*
[b] *University of Science and Technology of China, Hefei, Anhui, 230027, China*
[c] *Hefei University of Technology, Hefei, Anhui, 230009, China*

A R T I C L E I N F O

Article history:
Received 17 August 2018
Received in revised form
1 December 2018
Accepted 8 December 2018
Available online 1 January 2019

Keywords:
Hydrogen fusion energy systems
Liquid blanket
In-box LOCA
LBBFoam

A B S T R A C T

Blanket is the strategic component in hydrogen fusion energy system, converting nuclear energy of hydrogen nuclei to thermal energy which could be further transported for the production of electricity. In order to investigate blanket transient behaviors induced by the in-box LOCA (Loss of Coolant Accident), a code named LBBFoam for high pressure compressible multi-phase flow is developed based on OpenFOAM, which is capable of simulating accident-induced pressure wave propagation in the blanket module. Two classic one dimension shock tube cases were simulated to verify the code. With this code, three scenarios with 8 MPa helium injection into PbLi in a blanket-like container were analyzed to capture pressure oscillation and bubble transportation characteristics. It is found that the maximum pressure in the PbLi zone exceeds and even doubles the helium injection pressure due to the reflection and superposition of pressure waves. This suggests that the traditional structural safety design limits of helium cooled PbLi blanket, which is usually set as the operating pressure of helium coolant, would be too low considering pressure wave superposition. This code will provide an assessment tool for the structural safety of blanket.

Introduction

Blanket is well recognized as a key energy conversion component for hydrogen fusion energy system [1,2], converting nuclear energy of hydrogen nuclei to thermal energy which could be further transported for the production of electricity. The liquid PbLi blanket is one of the most promising blanket concepts [3–5], and the typical liquid blanket concept in China is the DFLL blanket (Dual-Functional Lead Lithium blanket) [6,7], which was originally developed by the Institute of Nuclear Energy Safety Technology, Chinese Academy of Sciences. This blanket has two coolants to transport the nuclear heating, including PbLi and helium, and PbLi is also the tritium breeding and neutron multiplication material. The blanket structure is made of China Low Activation Martensitic (CLAM)

* *Corresponding author.*
E-mail address: zhibin.chen@fds.org.cn (Z. Chen).
https://doi.org/10.1016/j.ijhydene.2018.12.066

Nomenclature and abbreviations

α_i	Volume fraction of phase *i*
ρ_i	Density of phase *i*
ρ_0	Reference density at standard atmospheric pressure
$\vec{U}$	Velocity vector
p	Pressure
p_{pb}	Pressure of PbLi
p_{atm}	Standard atmospheric pressure
μ	Dynamic viscosity
$\vec{g}$	Acceleration of gravity
E	Energy
K^{eff}	Thermal conductivity
LOCA	Loss of coolant accident
CFD	Computational fluid dynamics
DCLL	Dual-cooled lead lithium
DEMO	Fusion demonstration reactor
DFLL	Dual-functional lead lithium
HCLL	Helium cooled lead lithium
MHD	Magnetohydrodynamics
PbLi	Lead-lithium eutectic alloy
TVD	Total variation diminishing schemes
VOF	Volume of fraction
WCLL	Water cooled lead lithium

steel, with the thickness of about 30 mm filled with so many high pressure (8 MPa) helium tubes. And high temperature (~700 °C) PbLi flows slowly with the pressure of 2 MPa inside the blanket structure converting the neutron energy to the nuclear heating and meantime breeding tritium and multiplying neutrons. The total size of blanket is about 0.5 m width, 0.5 m length, and 2 m height, but it depends on the experimental and demonstration reactor where blanket would be tested on [8,9]. So far, comprehensive research has been conducted on the DFLL blanket, such as the coolant compatibility test [10], neutronics simulation and experiment [11–13], and the development of structure material [14–16].

In liquid PbLi blanket, helium thin tubes could fail under coupled loads of high pressure, high temperature PbLi MHD [17] (magnetohydrodynamics) corrosion, and high energy neutron irradiation, which leads to the occurrence of in-box LOCA (Loss of Coolant Accident). Injection of high pressure helium into low pressure PbLi zone seriously threatens the integrity of blanket structure, and causes the release of radioactive inventories. Thus, in-box LOCA is generally considered as a design basis accident for blanket safety [18].

When in-box LOCA happens, high-pressure helium injects into PbLi flow channel, forming a complex two-phase MHD flow. The pressure rises rapidly in PbLi flow channels, and peak pressure is very likely to exceed the injection pressure of helium due to the superposition of pressure waves. Therefore, it is of great significance to capture the propagation of pressure shock wave in the blanket [19].

An experimental study of WCLL (Water Cooled Lead–Lithium) blanket in-box LOCA was conducted using the LIFUS5 facility in ENEA [20], and the injection of high-pressure water into PbLi caused a transient pressure increase in PbLi area, due to the hammer effect. Simulation results by SIMMER-III code showed that injection of water flashed into PbLi and caused a sudden pressurization of 12.7 MPa at 20 ms. The experimental pressurization time was a little slower because of early rupture of cap.

A similar accident was also analyzed for the DCLL (Dual-cooled Lead Lithium) TBM with MELCOR [21], but the pressure shock wave and hammer effect caused by high-pressure helium injection were not considered in the analysis. The calculation by system code MELCOR suggested that the injection of high-pressure helium into breeding zones increased the pressure to the injection pressure of helium (8 MPa) in 100 ms and quickly reduced to 0.1 MPa. The rupture disk of the drain tank opened under 8 MPa and the pressure rose to 0.15 MPa in 4 s. No significant venting of the tank occurred and the port cell pressure remained constant.

In China, the in-box LOCA of DFLL blanket was recently analyzed by using a modified RELAP version [22]. Due to the channel rupture, the peak pressure of 7.8 MPa was found inside the blanket, but reflections and superposition of pressure waves were not captured. Very shortly after the accident (~0.0078 s), rupture valve opened due to the dramatic increase of pressure in PbLi channel, and lead-lithium started to be dumped into a tank. And then the helium pressure began to decrease till the entire system pressure below 2 MPa, with no more helium flow.

In Europe, HCLL (Helium Cooled Lead Lithium) box was designed to withstand pressure of 8 MPa [23]. A simulation of HCLL in-box LOCA experiment on THALLIUM was conducted using RELAP5-3D in ENEA, which showed that the peak pressure of the loop is below 7 MPa [24]. Both analysis of system codes MELCOR and REALP showed a pressure increase not exceeding the injection pressure of helium, which is different from the pressure superposition phenomena of hammer effect in coolant loop of fission power plant [25]. To further investigate the pressure wave in complex channel of blanket, 3D CFD tools other than the system code are needed [26].

Therefore, one-dimension system codes (e.g. RELAP, MELCOR, SIMMER) are not capable of simulating the reflection and superposition of pressure waves in the complex three-dimension liquid blanket box. More importantly, the pressure peak by the one-dimension system codes would be predicted much lower than the actual peak pressure, and a much lower safety limit for blanket structural design may be adopted giving rise to a big safety concern.

In this paper, a CFD code for high-pressure compressible multi-phase flow, named LBBFoam, was developed based on OpenFOAM [27], with the aim to reasonably capture the high pressure wave propagation behavior in the liquid blanket under in-box LOCA. Classical shock tube cases were simulated to verify the code. Then the pressure wave and bubble transportation behaviors induced by the injection of 8 MPa helium into PbLi in blanket-like containers were simulated and analyzed.

Governing equations and numerical methods

In the multi-phase model of LBBFoam, a conventional VOF method [28] is used for capturing the interface for PbLi and helium flows, which can model two fluids by solving a set of momentum equations and tracking the volume fraction of each fluid in the whole domain. Note that the VOF model is based on the assumption that two fluids do not permeate each other, and it is the case for the PbLi-helium flow. Moreover, variables and properties in any given control volume represent either pure PbLi or helium, or a mixture of phases, depending on the volume fraction. The governing equations include volume fraction equation, momentum equation, energy equation, and state equation.

The volume faction equation

$$\frac{\partial \alpha_i \rho_i}{\partial t} + \nabla \cdot \left(\alpha_i \rho_i \vec{U} \right) = 0 \tag{1}$$

where i = 1 or 2, representing phase 1 or phase 2. α_i, ρ_i represent the volume fraction, density of phase i. $\vec{U}$ represents the velocity vector. The volume fraction can be computed based on the following constraint:

$$\alpha_1 + \alpha_2 = 1 \tag{2}$$

The momentum equation:

$$\frac{\partial \rho \vec{U}}{\partial t} + \nabla \cdot \left(\rho \vec{U}\vec{U} \right) = -\nabla p + \nabla \cdot \left[\mu \left(\nabla \vec{U} + \nabla \vec{U}^T \right) \right] + \rho \vec{g} \tag{3}$$

where p represents pressure, μ is dynamic viscosity, and $\vec{g}$ is gravitational acceleration. The property of ρ stands for average density contributed by two phases:

$$\rho = \alpha_1 \rho_1 + \alpha_2 \rho_2 \tag{4}$$

All other properties (for example, viscosity, effective thermal conductivity) are computed in this manner.

The energy equation:

$$\frac{\partial \rho E}{\partial t} + \nabla \cdot \left[\vec{U}(\rho E + p) \right] = \nabla \cdot \left(K^{eff}\, \nabla T \right) \tag{5}$$

where K^{eff} is thermal conductivity. Energy E is treated as a mass-averaged variable:

$$E = \frac{\sum_{i=1}^{2} \alpha_i \rho_i E_i}{\sum_{i=1}^{2} \alpha_i \rho_i} \tag{6}$$

PbLi state equation [29–32] is important for the pressure wave speed, which is shown as follows:

$$p_{pb} = A\left(\rho_{pb} - \rho_0\right)^2 + B\left(\rho_{pb} - \rho_0\right) + C \tag{7}$$

where.

$$\rho_0 = 11340\ kg/m^3$$
$$A = 922.9\ m^5 kg^{-1} s^{-2}$$
$$B = 4368100\ m^2 s^{-2}$$
$$C = p_{atm} = 101325\ kg\ m^{-1} s^{-2}$$

p_{pb} is the pressure of PbLi and ρ_0 is reference density at standard atmospheric pressure. A, B and C are polynomial coefficients. p_{atm} represents standard atmospheric pressure.

To capture the pressure shock, a second order TVD scheme is applied to the convective term [33] of momentum equation. The time term is in an implicit Euler discrete scheme, and the diffusion term is in a linear orthogonal format.

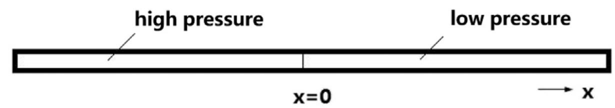

Fig. 1 – 1D shock wave tube model of single gas phase.

1D shock wave tube with air

A classic case of one-dimension shock tube was used to verify the code with single phase, and the model is shown in Fig. 1. Air, treated as ideal gas, was filled into the tube of length 0.2 m. The initial conditions are detailed in Table 1. A thin film in the middle of the tube (X = 0) separates the tube into two parts: the pressure of the left part is high pressure zone at 1 MPa and the right part is low pressure zone at 0.1 MPa. After the break of the thin film, shock wave propagates to the right side, and rarefaction wave propagates to the left.

The comparison between calculation and theoretical solution of density, pressure and temperature is shown in Fig. 2. It is found that the code has very good capability to predict the rarefaction wave propagating in the high pressure area and to capture the discontinuous position of shock wave. The edges of the shock waves are somewhat smoothed by the addition of viscosity.

1D shock wave tube with helium-PbLi

Considering the great difference of the compressibility of gas and liquid phases, the pressure fluctuation of two-phase shock tube will be significantly different from that of single-phase shock tube. Another one-dimensional shock wave tube case of liquid PbLi and helium was chosen to verify the characteristic of pressure wave propagation of two-phase flow between helium and PbLi. As shown in Fig. 3, liquid PbLi and helium in a one-dimensional tube are separated by a film. The initial conditions are summarized in Table 2. The initial pressure of PbLi and helium is 2 MPa and 8 MPa, respectively. The helium space is large enough and assumed at constant pressure of 8 MPa. At time 0 s, thin film breaks and pressure wave of $\Delta P = 6$ MPa forms.

Pressure wave propagation at the left end and center of tube can be seen in Fig. 4. Both theoretical and simulation results show that the maximum pressure reaches 14 MPa. The pressure fluctuation in the lead-lithium center region has two steps and only one step at the left end due to different positions of shock wave superposition. As in the previous single phase shock tube case, the discontinuous shock waves are smoothed out by viscosity. These simulation results show good agreement with the theoretical results, which verifies the code capability to capture pressure wave propagation between helium and PbLi.

Table 1 – Parameters of 1D shock wave tube model.

	$x < 0$	$x \geq 0$
p	1 MPa	0.1 MPa
T	527 °C	27 °C
U	0 m/s	0 m/s

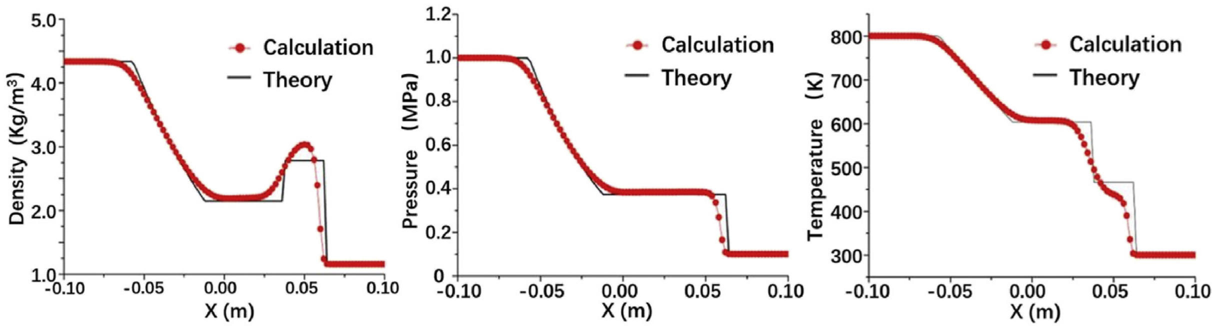

(a) Density (b) Pressure (c) Temperature

Fig. 2 – Comparison of numerical results and theoretical solutions (t = 0.1 ms).

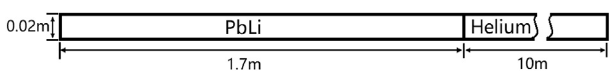

Fig. 3 – 1D shock wave tube model of PbLi and helium.

Multi-cycle of the pressure wave calculated is shown in Fig. 5. As time goes on, pressure wave will decay and the pressure at the center of the PbLi decays faster than the pressure at the end. The pressure oscillation in PbLi zone tends to be slighter and the step characteristics of pressure waves gradually disappear. In the cycles, a little mount of helium sprays into the PbLi area at the beginning and then flows back and forth across the interface.

Transient analysis of helium jet into PbLi

Three typical scenarios as indicated below was selected from many scenarios of in-box LOCA in various liquid blanket designs, to analyze transient behaviors after the injection of 8 MPa helium into PbLi in blanket-like containers.

Helium jet into an infinite PbLi zone

The first scenario is the high pressure helium injection into the two-dimension infinite PbLi zone. The shock wave propagation and helium bubble movement is simulated. In this scenario, the geometry model of PbLi is a 0.2 m × 0.2 m rectangular area and the helium jet nozzle diameter is 2 cm wide located at the bottom of the PbLi zone. Far-field boundary condition were set on the upper and both left and right sides of the PbLi zone. The initial pressure of PbLi is 2 MPa and the temperature is 590 °C. At the bottom of PbLi zone, the high pressure helium jet was set as 'Pressure-inlet' condition at 8 MPa with the temperature of 371 °C. High pressure helium was modeled as an ideal gas and properties of PbLi was calculated with Eq. (7) mentioned above.

Table 2 – Parameters of 1D shock wave tube model.

	$x < 1.7$ m	$x \geq 1.7$ m
p	2 MPa	8 MPa
T	400 °C	600 °C
U	0 m/s	0 m/s

Pressure wave propagation in the PbLi zone is shown in Fig. 6. Pressure wave travels much faster in the liquid phase than it does in the gas phase. A spherical wave spread forward rapidly through the PbLi zone. The propagation speed of pressure waves in PbLi is close to 1700 m/s. The pressure wave spread over the calculation PbLi area in 120 us. When the pressure wave propagates from the high-pressure helium to the two-dimension infinite lead-lithium area, the pressure wave is not a discontinuous shock wave but a continuous pressure wave. Transition area can be clearly seen between the low pressure area and the high pressure area. Since the computation model is a flat two-dimension rectangular region, there are no complicated geometric shapes or obstacles, and thus no superposition of pressure wave happens. The maximum pressure of PbLi zone is the same as the initial pressure of helium (8 MPa).

Bubble motion of high pressure helium jet into the liquid PbLi zone is shown in Fig. 7. For the high sound speed of PbLi, the pressure wave spreads in microsecond level. But the motion of helium bubble under buoyancy force is in second level. Therefore, when the bubbles start to enter the PbLi zone, the pressure in the PbLi region is already stable at 8 MPa. At the

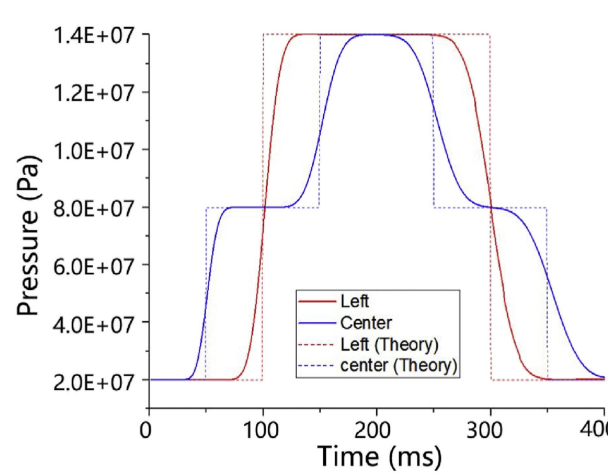

Fig. 4 – Pressure wave propagation at the left end and center of tube.

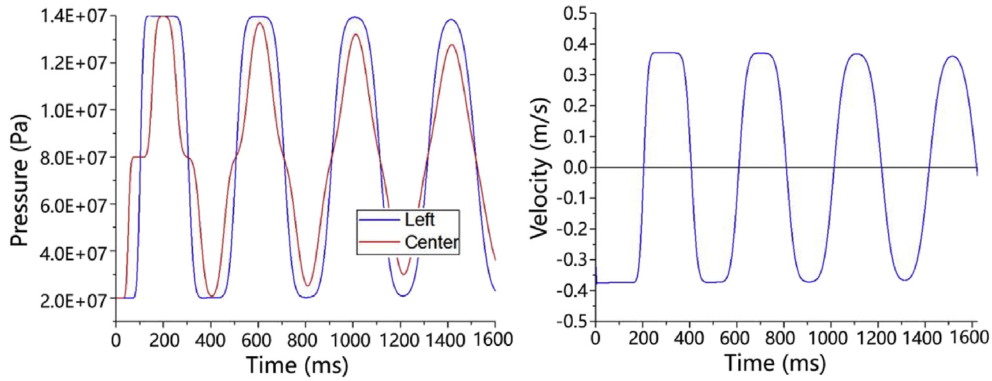

(a) Pressure oscillation (b) Velocity of helium at interface

Fig. 5 – Multi-cycle of the pressure wave between helium and PbLi.

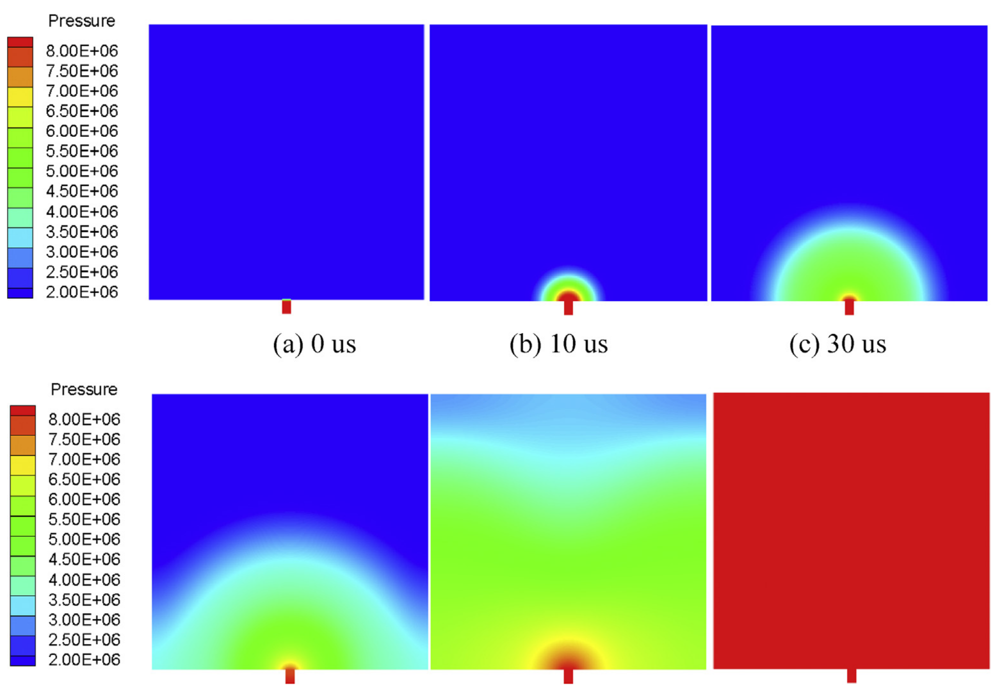

(a) 0 us (b) 10 us (c) 30 us

(d) 50 us (e) 100 us (f) 200 us

Fig. 6 – Shock wave propagation of helium jet into an infinite PbLi zone (Unit: Pa).

beginning, the interface between helium and PbLi is almost stationary, and begins to deform due to the Rayleigh-Taylor instability. At 0.05 s, bubbles move upward under buoyancy force and PbLi flows downward into the helium nozzle, blocking part of the nozzle. At 0.2 s, small bubbles start moving into the PbLi zone. At 0.4 s, the bubble continues to rise but starts breaking into several small bubbles. Subsequently, as more helium enters PbLi zone, the volume of the gas phase gradually increases and the distribution of bubbles becomes more complex. In this condition, no large cavities are formed, and the difference of bubble size is relatively small with the maximum of 5 cm.

Therefore, when the high-pressure helium injects into the infinite PbLi zone, the pressure of two phases will reach equilibrium before helium entering PbLi. After the pressure balance, the helium will only float upwards under the effect of buoyancy, and the bubbles generated will burst in the rising process, resulting in smaller bubble sizes in PbLi.

Helium jet into a finite PbLi zone

The second scenario is to simulate the pressure oscillation and movement behavior of high pressure helium gas in a limited area. The geometry model is similar to the first one, which is also a 0.2 m × 0.2 m rectangular area of PbLi, but the boundary conditions are different. The boundaries are all set to 'Wall', which means the pressure waves can reflect back and form superposition in PbLi zone. In the center of PbLi zone, there is a high pressure helium bubble with the diameter of 5 cm. The pressure of helium and PbLi

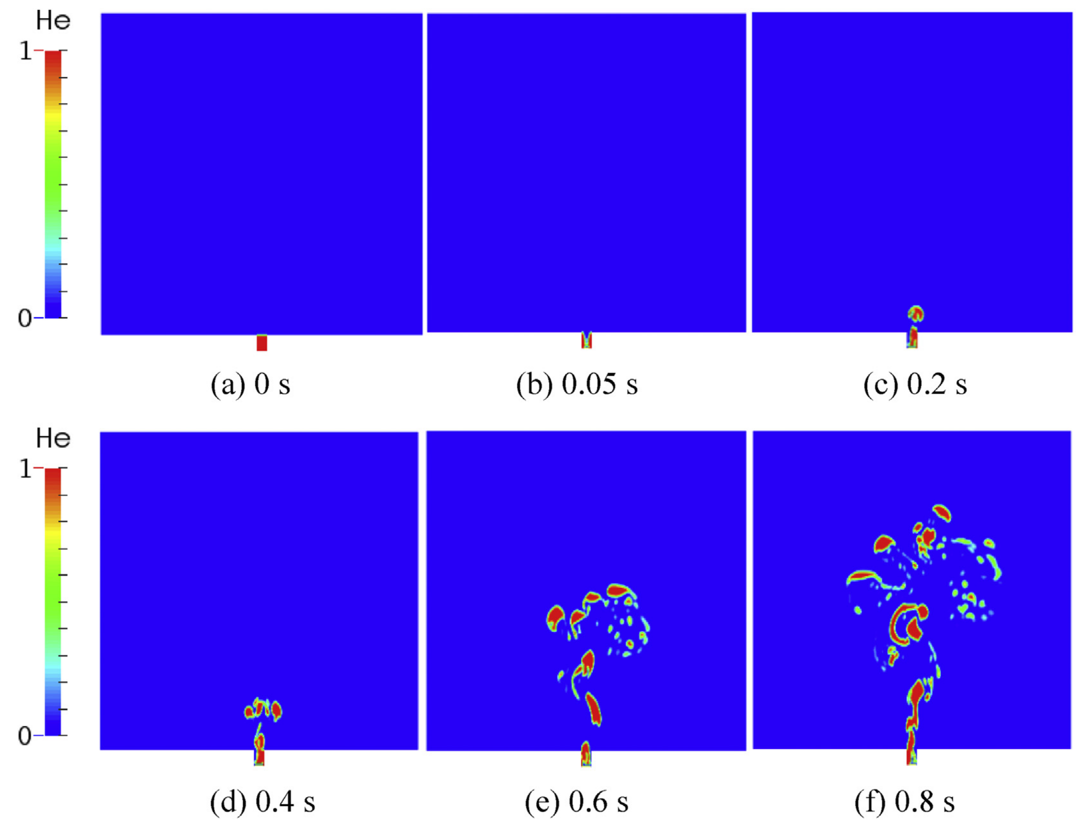

Fig. 7 – Bubble motion of helium jet into infinite liquid PbLi.

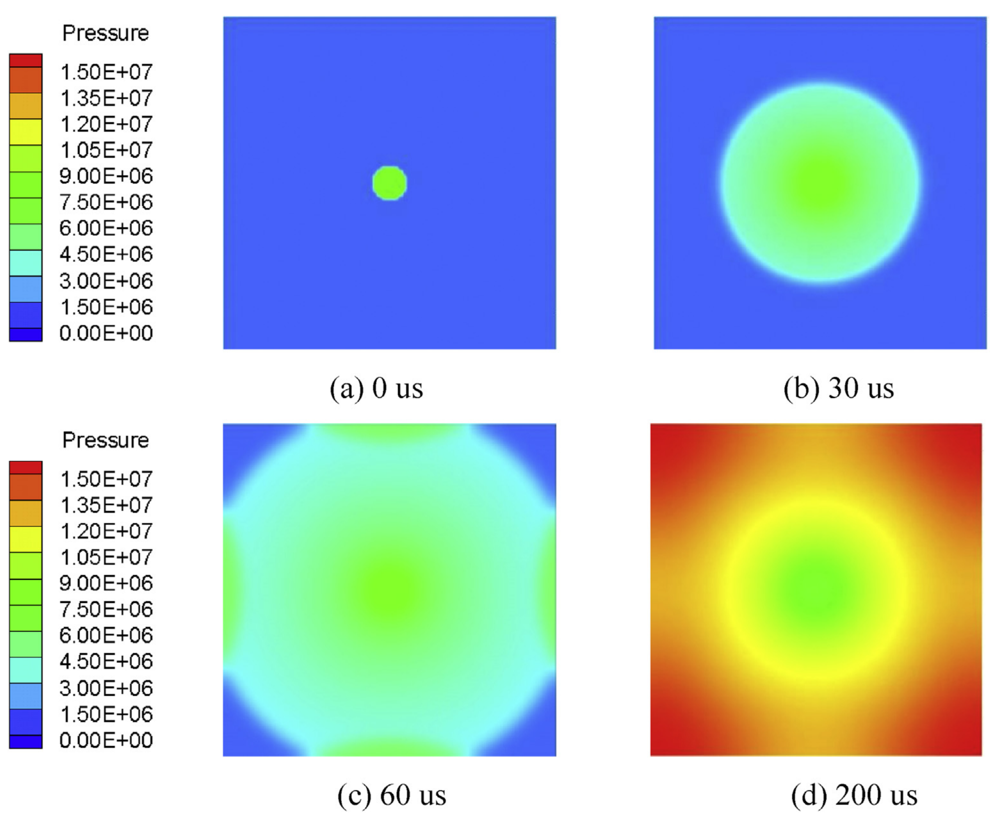

Fig. 8 – Pressure wave propagation of helium jet into the finite PbLi zone (Unit: Pa).

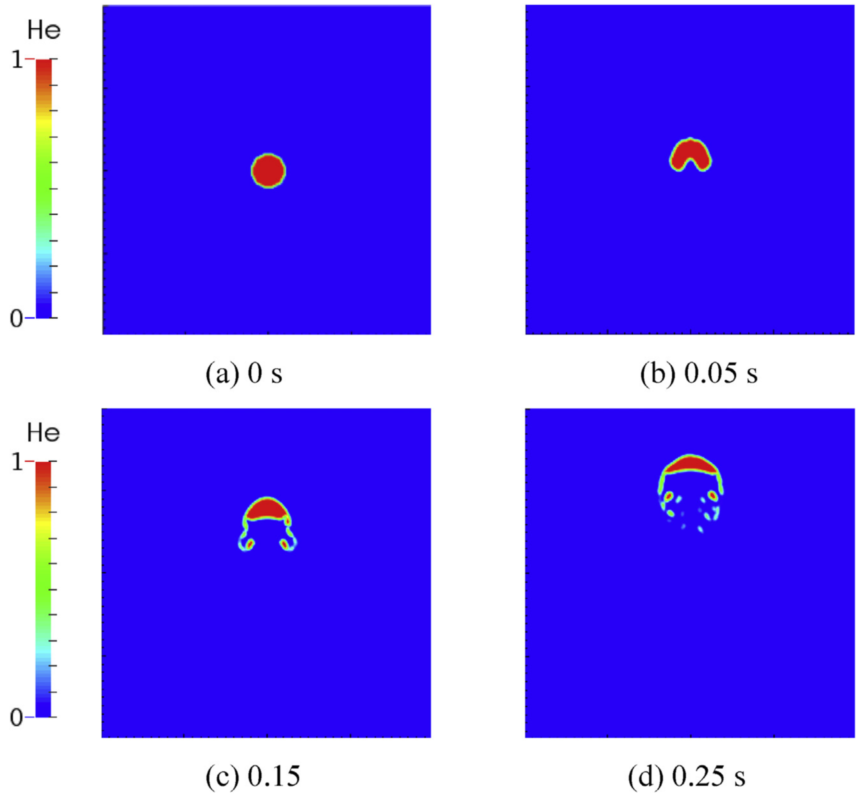

Fig. 9 – High pressure helium bubble in the liquid PbLi pool.

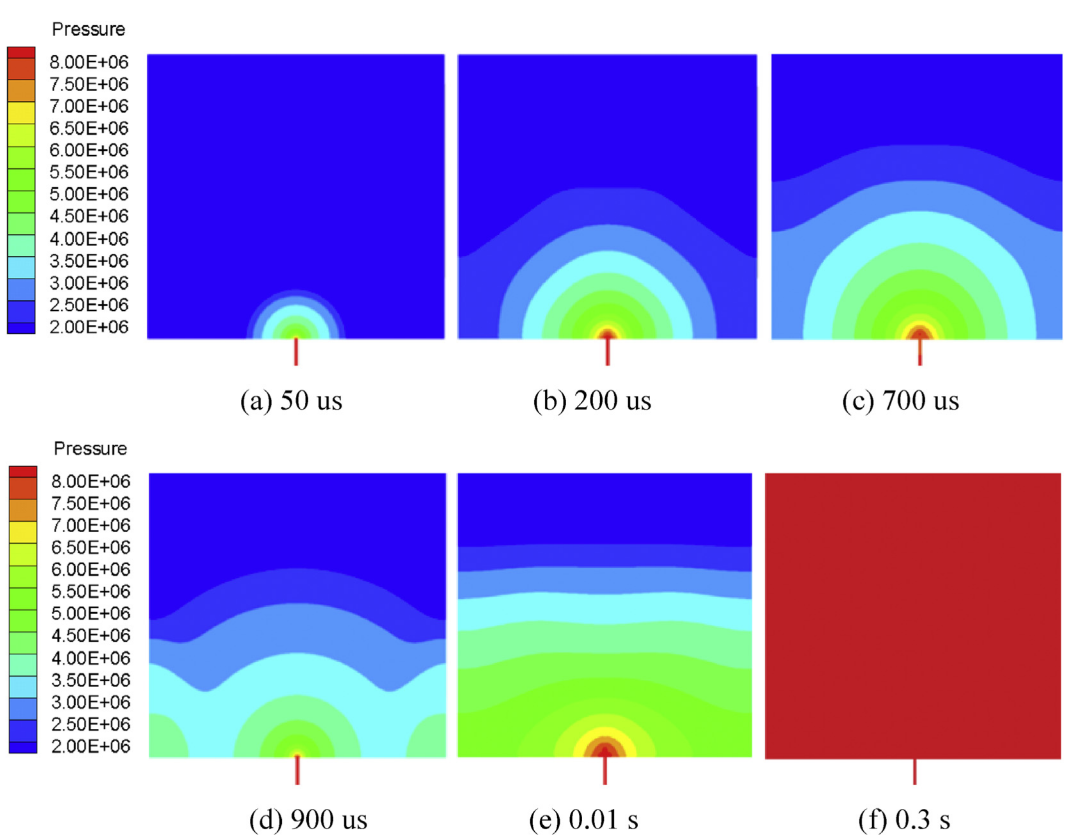

Fig. 10 – Pressure wave propagation of helium jet into finite PbLi area with top gas space (Unit: Pa).

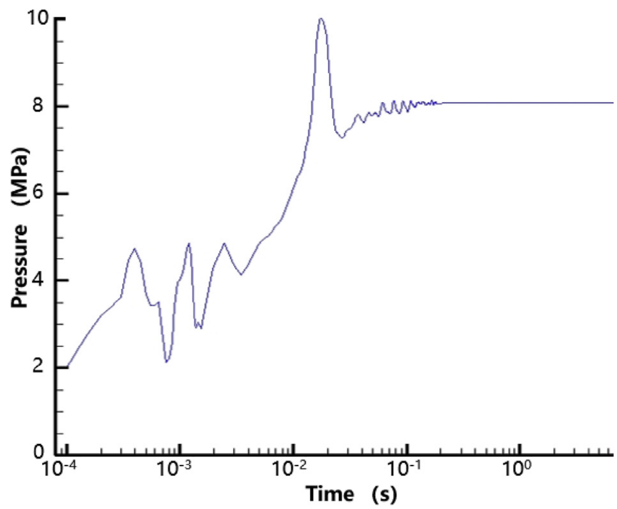

Fig. 11 – Pressure oscillation near side wall of PbLi zone.

are 8 MPa and 1MPa. The temperature of helium and PbLi is 371 °C and 590 °C.

The process of pressure wave propagation in PbLi zone is shown in Fig. 8. Under the high pressure of helium bubble, a spherical pressure wave formed and spread outward rapidly. At the same time, a rarefaction wave propagates internally in the helium bubble. At 60 us, the pressure waves reach the boundary walls and begin to reflect from the walls, and then distorts the original spherical wave front. Due to the reflection and superposition of the waves, the pressure peak appears at the corners and also the central area. The peak pressure reaches about 16 MPa, which is almost twice of initial helium pressure. Compared with the results in the first scenario, the reflection and superposition of pressure waves have significant influence on the pressure peak. The pressure oscillations continue at 200 us and the time to reach the pressure balance varies significantly from the first scenario.

The motion of helium bubble is still lagging behind the propagation of pressure wave, as shown in Fig. 9. When the helium bubble begins to deform, the pressure in the PbLi zone is near equilibrium. The reason for motion of helium bubble is buoyancy force. At 0.05 s, bubble moves upward under the buoyancy force and transforms into crescent shape due to the Rayleigh-Taylor instability. At 0.1 s, the helium bubble becomes thinner, longer and more curved. At 0.15 s, both ends of the bubble become instable and small bubbles begin to form due to the instability. At 0.25 s, many smaller bubbles appear in the wake of bigger bubble.

Helium jet into a finite PbLi pool with a gas space

For blanket system, the internal space is not completely filled with liquid-phase of PbLi, and there are devices within the gas-phase space such as expansion box and voltage stabilizer. The influence of gas phase space on in-box LOCA should also be considered.

The third scenario is a simplified model of blanket system to simulate the basic phenomenon of pressure wave propagation. The calculation model is a 0.5 m × 0.5 m rectangle area of PbLi and helium, and the boundary conditions was all set to 'Wall'. One fifth of the zone at the top is filled with 2 MPa helium and the remaining part is patched with 2 MPa PbLi. And at the bottom of PbLi zone, there is a high pressure helium nozzle with 'Pressure-inlet'

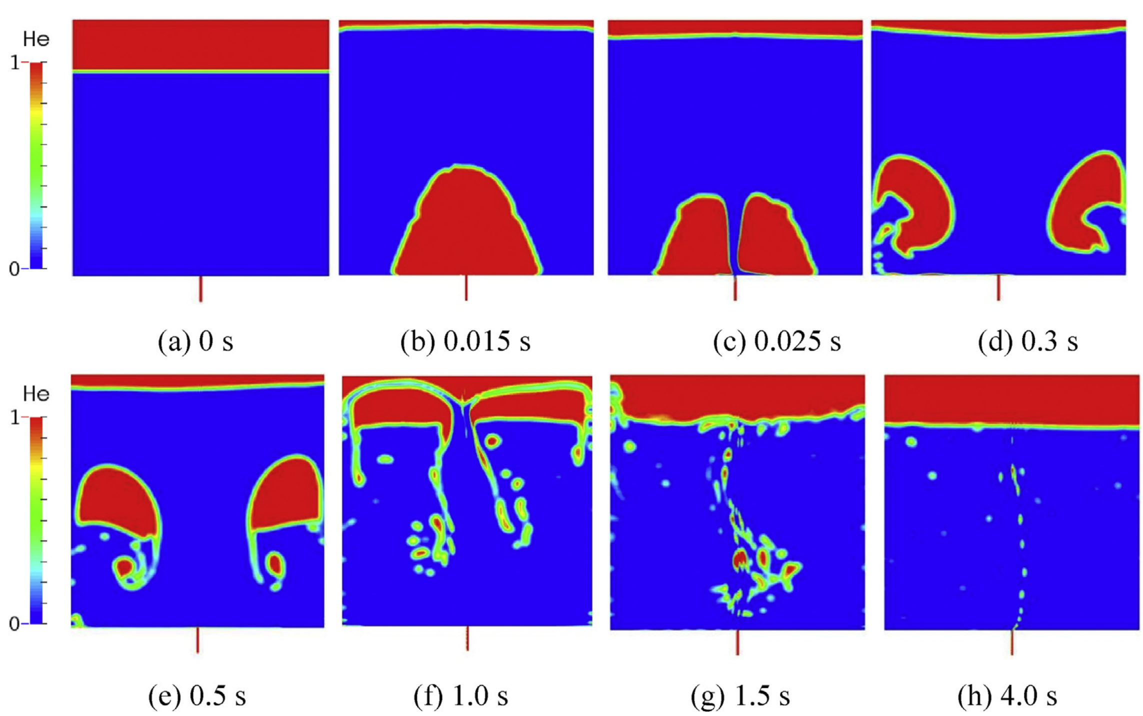

Fig. 12 – Bubble motion process of high pressure helium jet with top helium space.

condition at 8 MPa. The temperature of PbLi is 590 °C and the helium temperature is 371 °C.

The existence of the gas space greatly absorbed the pressure wave. As shown in Fig. 10, there is an obvious pressure gradient between top helium area and helium jet at 0.01 s, and it takes about 0.3 s to achieve pressure balance, which is much longer than the time reaching pressure balance in pure PbLi pools (~100 us). The peak of pressure oscillation near side wall reaches about 10 MPa, as indicated in Fig. 11.

The bubble motion process is complicated and could be described in the following stages, as shown in Fig. 12.

1) Pressure propagation stage in early 0.0002 s: as the sound velocity of PbLi reaching around 1700 m/s, the pressure wave quickly propagates in the PbLi area immediately after the helium injected.
2) Pressure oscillation stage in early 0.01 s: The pressure gradient between top helium area and helium jet forms. Pressure wave at the lower part reflects on the side wall and superposes to reach 10 MPa, as also shown in Fig. 11.
3) Helium bubble formation stage in early 1 s: with the expansion of high pressure helium jet, a single large (about 30 cm in diameter) helium bubble forms, and compresses top helium area to reach pressure balance. The single large helium bubble splits into two bubbles of medium size and flows upward to fuse into top helium area.
4) Helium bubble motion stage: after 1 s, the pressure balance is built between top helium area and helium jet. The flow field in the container gradually stabilizes, and continuous small helium bubbles formed by the jet tube flow upward under the buoyancy force.

Conclusion

In this contribution, LBBFoam was developed based on the OpenFOAM platform, aiming to understand transient behaviors in the liquid blanket induced by the in-box LOCA. The corresponding verification was made with an ideal gas shock wave tube case and a helium-PbLi shock wave tube case, and the calculation results were in good agreement with theoretical solution, indicating the code capability to simulate pressure wave propagation and bubble motion of helium-PbLi compressible flows.

Three typical scenarios of transient behaviors after the injection of 8 MPa helium into PbLi were simulated, and here are the findings:

(1) Helium jet into an infinite PbLi zone: in early stage, the shock wave spreads over the calculated PbLi area and soon achieves pressure equilibrium, while in later stage, bubble starts moving upward under buoyancy force. Considerable amounts of helium bubbles were observed in the PbLi zone after 0.4 s.
(2) Helium jet into a finite PbLi pool: pressure wave reflects on walls and superposition of pressure wave leads to the peak pressure of around 16 MPa, which is almost twice of initial helium pressure.
(3) Helium jet into a finite PbLi pool with a gas space: the existence of the gas space greatly absorbs the pressure wave and it takes longer time to reach pressure balance. The peak pressure of 10 MPa also exceeds the helium injection pressure. A large bubble in the jet forms and then compresses the top helium area to increase its pressure. After the balance process, continuous small helium bubbles form near the jet tube flowing upward under the buoyancy force.

Therefore, it is clearly indicated that the maximum pressure in the PbLi zone will exceed the helium injection pressure of 8 MPa considering the reflection and superposition of pressure waves, and even double under finite containment scenario. This means that the traditional structural safety design criterion, which is usually set as the operating pressure of helium coolant, would be too low considering pressure wave superposition.

Comparing with one-dimension system code, the LBBFoam can simulate detailed behaviors of pressure wave propagation in blanket module, and could provide an assessment tool for the structural safety design of liquid blanket. For the next step, this code will be further verified and validated with experimental data of high pressure helium injecting into PbLi to ensure that its calculation results are qualitatively and quantitatively reliable. MHD modules will be embedded to analyze two phase MHD flow phenomena of in-box LOCA under strong magnetic field in the hydrogen fusion energy systems.

Acknowledgements

This work is supported by the National Magnetic Confinement Fusion Science Program of China [Grant No. 2014GB116000, 2014GB112002]; the Anhui Provincial Natural Science Foundation [Grant No. 1608085QA09]; and National Natural Science Foundation of China [Grant No. 51606206]. We would like to express our appreciation for the support from the members of FDS Team in this work.

REFERENCES

[1] Wu Y, Chen Z, Hu L, et al. Identification of safety gaps for fusion demonstration reactors. Nature Energy 2016;1:16154.
[2] Wu Y. Fusion neutronics. Springer; 2017.
[3] Aiello G, Dinechina GD, Foresta L, et al. HCLL TBM design status and development. Fusion Eng Des 2011;86:2129–34.
[4] Wong CP, Malang S, Sawan M, et al. An overview of dual coolant PbLi breeder first wall and blanket concept development for the US ITER-TBM design. Fusion Eng Des 2006;81:461–7.
[5] Lee DW, Hong BG, Kim Y, et al. Preliminary design of a helium cooled molten lithium test blanket module for the ITER test in Korea. Fusion Eng Des 2007;82:381–8.
[6] Wu Y. Design status and development strategy of China liquid lithium-lead blankets and related material technology. J Nucl Mater 2007;367:1410–5.
[7] Wu Y, FDS Team. Design analysis of the China Dual-Functional Lithium Lead (DFLL) test blanket module in ITER. Fusion Eng Des 2007;82:1893–903.
[8] Wu Y. Conceptual design of the China fusion power plant FDS-II. Fusion Eng Des 2008;83(10–12):1683–9.

[9] Wu Y, Jiang J, Wang M, et al. A fusion-driven subcritical system concept based on viable technologies. Nucl Fusion 2011;51(10):103036.
[10] Huang Q, Gao S, Zhu Z, et al. Progress in compatibility experiments on lithium-lead with candidate structural materials for fusion in China. Fusion Eng Des 2009;84:242–6.
[11] Wu Y. Development of high intensity D-T fusion neutron generator HINEG. Int J Energy Res 2018;42:68–72.
[12] Wu Y, Song J, Zheng H, et al. CAD-based Monte Carlo program for integrated simulation of nuclear system SuperMC. Ann Nucl Energy 2014;2:161–8.
[13] Wu Y. CAD-based interface programs for fusion neutron transport simulation. Fusion Eng Des 2009;84:1987–92.
[14] Huang Q. Status and improvement of CLAM for nuclear application. Nucl Fusion 2017;57. 086042.
[15] Huang Q, Baluc N, Dai Y. Recent progress of R&D activities on reduced activation ferritic/martensitic Steels. J Nucl Mater 2013;442:S2–8.
[16] Huang Q, Li C, Li Y, et al. Progress in development of China Low Activation Martensitic steel for fusion application. J Nucl Mater 2007;367:142–6.
[17] Smolentsev S, Moreau R, Bühler L, et al. MHD thermofluid issues of liquid-metal blankets: phenomena and advances. Fusion Eng Des 2010;85:1196–205.
[18] Abdou M, Morley NB, Smolentsev S, et al. Blanket/first wall challenges and required R&D on the pathway to DEMO. Fusion Eng Des 2015;100:2–43.
[19] Carloni D, Gonfiotti B, Paci S, et al. LOCA accident for the DEMO helium cooled blanket. Fusion Sci Technol 2015;68:353–7.
[20] Ciampichetti A, Ricapito I, Aiello A, et al. Water large leaks into liquid PbLi: first experimental results on LIFUS 5 facility. Fusion Eng Des 2003;69:563–7.
[21] Merrill BJ, Cadwallader LC, Wong CPC, et al. US dual coolant lead lithium ITER test blanket module preliminary safety report. Idaho National Laboratory Report; 2010. INL/EXT-10-18169.
[22] Sun Q, Peng T, Zhou Z, et al. Modification on the contact model of LiPb and non-condensable gas in RELAP/SCDAPSIM/MOD4.0 and application to LOCA of China DFLL-TBM. Fusion Eng Des 2018;134:35–42.
[23] Pinna T, Boccaccini LV, Salavy JF. Failure mode and effect analysis for the European test blanket modules. Fusion Eng Des 2008;83:1733–7.
[24] Utili M, Venturini A, Lanfranchi M, et al. THALLIUM: an experimental facility for simulation of HCLL In-box LOCA and validation of RELAP5-3D system code. Fusion Eng Des 2017;123:102–6.
[25] Lieberman P, Brown E. Pressure oscillations in a water-cooled nuclear reactor induced by water-hammer waves. J Fluid Eng 1960;82:901–7.
[26] Sun Q, Peng T, Zhou Z, et al. CFD simulation of pressure wave propagation in the helium coolant tube break accident of DFLL-TBM. Fusion Eng Des 2018;136:950–7.
[27] OpenCFD Ltd. OpenFOAM. 2018. https://openfoam.org.
[28] Hirt CW, Nichols BD. Volume of fluid (VOF) method for the dynamics of free boundaries. J Comput Phys 1981;39:201–25.
[29] Lindstrom M, Barsky S, Wetton B. Investigation into fusion feasibility of a magnetized target fusion reactor: a preliminary numerical framework. J Fusion Energy 2015;34:76–83.
[30] Valls DL, Sedano LA, Batet LE, et al. Lead–lithium eutectic material database for nuclear fusion technology. J Nucl Mater 2008;376:353–7.
[31] Stankus SV, Khairulin RA, Mozgovoi AG. An experimental investigation of the density and thermal expansion of advanced materials and heat-transfer agents of liquid-metal systems of fusion reactor: lead-lithium eutectic. High Temp 2006;44:829–37.
[32] Ueki Y, Hirabayashi M, Kunugi T, Yokomine T, et al. Acoustic properties of Pb-17Li alloy for ultrasonic Doppler velocimetry. Fusion Sci Technol 2009;56:846–50.
[33] Bruner S. Parallelization of the Euler equations on unstructured grids. Ph.D. thesis. Virginia Polytechnic Institute and State University; 1996.